μ-DSMC: A general viscosity method for rarefied flow

M. N. Macrossan

Center for Hypersonics, Division of Mechanical Engineering, University of Queensland, Australia 4072

E-mail: M.Macrossan@uq.edu.au

A modified DSMC method for rarefied flows is described, by which *any* viscosity law $\mu = \mu(T)$ may be simulated, including experimental data directly. The collision cross-section of a simple collision model is made to vary from cell to cell, based on the time-averaged cell temperature and the required viscosity at that temperature. The new method is tested in two different flows: high speed Couette flow and a plane 1D shock. For Couette flow, the shear stress and heat transfer, calculated from the velocity distribution, agree with the theoretical values calculated from the flow gradients and the theoretical transport coefficients. For the 1D shock, the new method is compared with the generalized hard sphere (GHS) model. The new method produces profiles of density and temperature which are generally indistinguishable from the GHS results except for a deviation in the T_x temperature component in a small region ahead of the shock. For the worst case the deviation is 4.6%, but it can be reduced by basing the imposed viscosity on the maximum component of kinetic temperature rather than the mean kinetic temperature. The new method is shown to be insensitive to the number of simulator particles used in each cell.

Three translational degrees of freedom are considered. However, because μ-DSMC is based on a hard sphere or VHS cross-section, it is compatible with the most commonly used Borgnakke-Larsen model for translational-rotational energy exchange.

Key Words: rarefied flow, numerical simulation (65C), DSMC, viscosity method, Sutherland viscosity, molecular dynamics (82A71)

1. INTRODUCTION

Bird's Direct Simulation Monte-Carlo method [2] is the standard computational method for rarefied flows, where the governing equation is the Boltzmann equation. In DSMC the flow is represented by a large number of simulator particles and the evolution of the flow is tracked by calculating the motion of these particles and their collisions amongst themselves and with any boundaries. The simulation is

advanced in time steps Δt during which the convection and collision calculations are de-coupled. After the particles are moved in collisionless flight, binary collisions are calculated between some of the particles, at a rate which reflects the collision probability for the particular collision cross-section used. Although the collision partners are near neighbours, they are not necessarily within one particle diameter. Post-collision velocities are calculated for the given relative speed of collision and a randomly chosen set of impact parameters.

The most common collision model now used in DSMC calculations is the variable hard sphere (VHS) model; the total collision cross-section varies with relative velocity in the same manner as for an inverse power repulsive potential, but the scattering is as for hard spheres - all directions of the post-collision relative velocity are equally likely. The first DSMC application of this combination of hard sphere differential cross-section and a variable total cross-section can be found in the papers of Borgnakke and Larsen [3] [13] [4], and later by Erofeev and Perepukhov [7] and Bird [1]. The Chapman-Enskog viscosity of the VHS collision model is a power law

$$\mu\left(T\right) = \mu_r \left(\frac{T}{T_r}\right)^{\frac{1}{2}+\upsilon},$$

where μ_r is the viscosity at a reference temperature T_r. This viscosity law matches that for a molecule displaying an inverse power repulsive intermolecular potential $U\left(r\right) \propto r^{-\alpha}$, where $\alpha = 2/\upsilon$.

The viscosity of real gases can be matched by a power law over a small temperature range only, because the long range attractive forces (the van der Waals forces) are ignored. More realistic is the Sutherland potential which combines a short range hard sphere repulsion with a long range inverse 6^{th} power attractive potential. The viscosity of the Sutherland potential is given by

$$\mu\left(T\right) = \mu_r \left(\frac{T}{T_r}\right)^{\frac{1}{2}} \frac{1+T_s/T_r}{1+T_s/T} \tag{1}$$

where the temperature T_s is a measure of strength of the attractive potential. With $T_s = 142$ K the Sutherland law fits the experimental viscosity data for argon (Kestin *et al.* [10]), reasonably well up to $T = 10T_s = 1420$ K, at which point the Sutherland viscosity is 8% less than the experimental data. In contrast, a power law viscosity is a poor representation of the experimental data over the same range. Fig. 1 shows this in exaggerated form, by comparing the Sutherland viscosity with that of the two extremes of the VHS collision model: $\upsilon = 0$ (the hard sphere molecule with constant cross-section) and $\upsilon = \frac{1}{2}$ (a 'Maxwell cross-section'). All three viscosities are set equal at $T = T_s$, but deviate markedly at high temperatures.

An intermediate value of υ could give a 'compromise' representation of the viscosity data over the temperature range shown in Fig. 1, but a different value of υ must be selected for each flow situation. A collision model based on a realistic potential can give a good representation of the viscosity of a typical gas over a wide range of temperature. For example Davis *et al.* [6] calculated and stored the deflection angles for the Morse potential for a large array of possible impact parameters and used a table look-up as required for each collision. Special procedures had to be used for impact parameters which exceeded the bounds of the array. While this

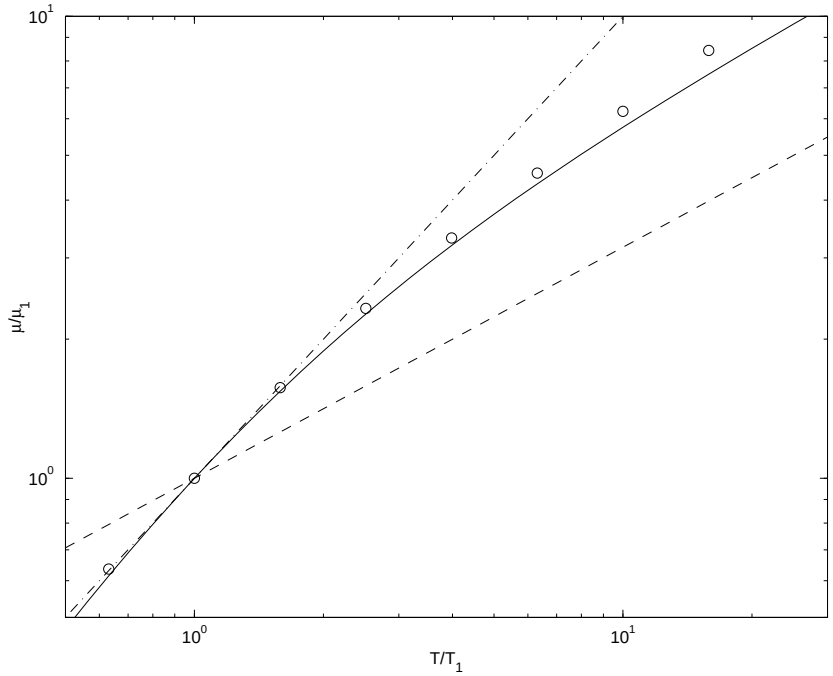

FIG. 1. Viscosity μ/μ_r *vs.* T/T_r for: —-, Sutherland, Eq. 1 ($T_s = T_r$); – –, hard sphere $\mu/\mu_r = (T/T_r)^{\frac{1}{2}}$; · – ·, linear law $\mu/\mu_r = T/T_r$. ∘ argon data Kestin *et al.* [10] $T_r = 142$ K, $\mu_r = 1.129 \times 10^{-5}$ Nm^{-1} s^{-1}.

'look-up' approach would be more manageable and accurate with present day computers, as might be exact calculations for realistic potentials for every collision as it occurs (Koura and Matsumoto [11]), it would be better to have a collision model as simple to implement as VHS and which produced a realistic viscosity law.

Here we describe such a simple method, called 'viscosity-DSMC' or μ-DSMC, by which a simple collision cross-section can be used to simulate *any* realistic viscosity law, including one based on empirical data. This is achieved by adjusting the parameters of a simple collision model on a cell by cell basis, based on the time-averaged temperature in each cell, and the required viscosity at that temperature. In the first example we assume a hard sphere (constant cross-section) collision probability in each cell, but achieve a Sutherland viscosity law by making the cross-section depend on the local cell temperature. In the second example we use a collision probability which corresponds to a 'soft' variable hard sphere cross-section with a fixed value of υ, but achieve a realistic viscosity law by making the reference size of the VHS cross-section depend on the cell temperature.

2. μ-DSMC: VARIABLE TEMPERATURE CROSS-SECTION

The Chapman-Enskog viscosity [5] for hard sphere molecules is

$$\mu = \frac{5m\pi^{\frac{1}{2}}}{16}\frac{(RT)^{\frac{1}{2}}}{\sigma}, \tag{2}$$

where σ ($= \pi d^2$, where d is the sphere diameter) is the total collision cross-section, m is the molecular mass and R is the ordinary gas constant. To produce a variation

of viscosity which deviates from the hard sphere law the total cross-section must vary from cell to cell based on the local time-averaged kinetic temperature $\bar{T}$ in the cell; that is, in each cell, at each time step, a local molecular size is computed as

$$\sigma\left(\bar{T}\right) = \frac{5m\pi^{\frac{1}{2}}}{16}\frac{\left(R\bar{T}\right)^{\frac{1}{2}}}{\mu\left(\bar{T}\right)}. \tag{3}$$

The standard DSMC procedures for a hard sphere molecule are then applied in each cell, based on the local value of σ. Thus, in each cell the number of collision pairs considered is

$$N_p = \frac{1}{2}\,\bar{n}N\sigma g_{max}\Delta t,$$

where g_{max} is an estimate of the maximum possible collision speed in the cell, σ is given by Eq. 3, N is the number of particles in the cell and $\bar{n}$ is the time-averaged value of the local number density. Note that $\bar{T}$ is calculated for each cell at the same time as is $\bar{n}$ in standard DSMC. The extra computational effort is negligible; the necessary samples are available as part of the standard DSMC procedures for obtaining the final steady state.

A pair is accepted for collision if $g/g_{max} > R_f$, where R_f is a uniformly distributed random fraction. The number of collisions accepted is

$$N_{coll} = \frac{\bar{g}}{g_{max}}N_p = \frac{1}{2}\,nN\sigma\bar{g}\Delta t,$$

where $\bar{g}$ is the average collision speed. The collision rate is

$$\nu = \frac{2N_{coll}}{N\Delta t} = n\sigma\bar{g},$$

or, with σ from Eq. (3),

$$\nu = \frac{5\pi}{16}\rho\bar{g}\frac{\left(R\bar{T}/\,\pi\right)^{\frac{1}{2}}}{\mu\left(\bar{T}\right)}.$$

Thus the local non-equilibrium collision rate depends on the velocity distribution, through $\bar{g}$, and the specified viscosity law $\mu\left(\bar{T}\right)$. The collision probability need not be $\propto g$ (as for a hard sphere total cross-section) but can be taken as $\propto g^{1-2/\upsilon}$, as for the VHS total cross-section (see §5).

3. COUETTE FLOW

Bird [2] has used a simulation of high speed Couette flow to check the viscosity and thermal conductivity for the VHS collision model. Here we do a similar thing to demonstrate that the μ-DSMC can produce a variation of viscosity given by Eq. 1, even though a hard sphere collision model is used locally in each cell. We consider molecules with three translational degrees of freedom only, so the specific heat at constant pressure is $C_p = 5R/2$. The viscosity law for μ-DSMC was imposed by using Eq. 1 to set the cross-section, via Eq. 3. The theoretical thermal conductivity is given by $K\left(T\right) = \mu\left(T\right)C_p/Pr$, where Pr = 2/3 is the Prandtl number.

The geometry and boundary conditions for Couette flow are shown in Fig. 2. The gas is contained between two plates parallel to the x-axis separated by a distance

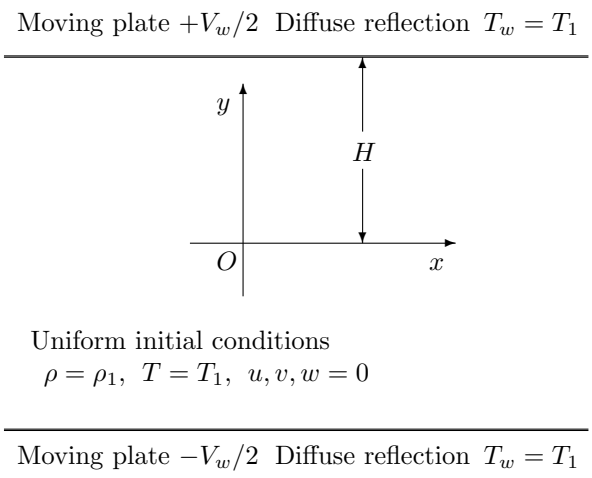

FIG. 2. Couette flowfield. Plane of skew symmetry at $y = 0$.

$2H$, moving in their own plane with speeds $\pm V_w/2$. There is a plane of skew symmetry mid-way between the plates, where the origin of the y-axis has been set. The flow extends infinitely in the x and z directions. Half the flow only, from $0 <= y <= H$ is simulated; simulator particles which cross the plane of skew symmetry are 'reflected' from the plane with their velocity and position vectors reversed.

The flow begins with a uniform gas density ρ_1 and temperature T_1 between the plates. The plate at $y = H$ begins to move at time $t = 0$, in the positive x-direction, with speed $V_w/2$. The plate temperature is held constant at $T_w = T_1$ and particles which collide with the plate are diffusely reflected. The wall speed ratio was $S_w = V_w/\left(2RT_w\right)^{\frac{1}{2}} = 3$.

The simulator gas density and molecular size, and therefore collision rate, are specified by the *nominal* mean free path

$$\lambda_1 = \frac{2\mu_1}{\rho_1 \bar{c}_1},$$

where $\bar{c}_1 = (8RT_1/\pi)^{\frac{1}{2}}$ is the mean thermal speed in the undisturbed gas. The Knudsen number, λ_1/H, was 0.01. The cell size was $\Delta y = H/200$ giving $\Delta y \approx 0.5\lambda_1$; 10 sub-cells per cell were used so that the average collision separation was $< 0.05\lambda_1$. There were 100 particles in each cell (on average) in the initial state. The decoupling interval was $\Delta t = \tau_1/5$, where $\tau_1 = \lambda_1/\bar{c}_1$ is a nominal collision time.

For similar calculations Bird [2] found that steady state was achieved after an elapsed time $375H/\bar{c}_1$. In the present calculations steady state was well established after an elapsed time of $400H/\bar{c}_1$ and samples taken after this time were used to derive the final time-averaged steady state. Samples of the flow were taken at intervals of $2\tau_1$. The simulation continued until the total sample size in each cell was $> 16 \times 10^6$ particles.

Steady state velocity and temperature profiles are shown in figure 3. All 'raw' profiles from the simulations have been smoothed by a moving average over five

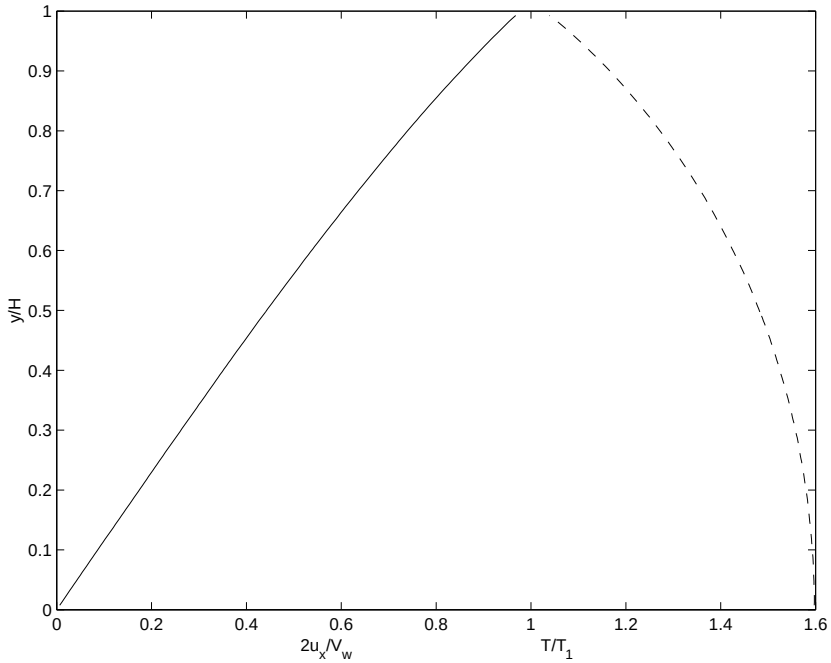

FIG. 3. Normalized velocity (—, $2u_x/V_w$) and temperature (– –, T/T_1) profiles for Couette flow for μ-DSMC with a Sutherland viscosity law ($T_s = T_1$). Plate separation is $2H$, $y = 0$ is plane of skew symmetry. $S_w = 3$, $\lambda_1/H = 0.01$. 200 cells, 10 sub-cells per cell. Sample size $> 16 \times 10^6$ in each cell. Each point in the profiles is an average over 5 cells.

cells (a distance $\approx 2.5\lambda_1$). The moving plate heats the flow; the temperature is a maximum at $y = 0$ and approaches the wall temperature at $y = H$.

The theoretical shear stress in the flow can be determined from the velocity gradient du_x/dy measured from the velocity profile, and the theoretical viscosity, $\mu(T)$ from Eq. 1, evaluated for the local flow temperature. The velocity gradient was taken as the slope of a line of 'least squares' best fit to the five adjacent smoothed values. The velocity gradient is shown in Fig. 4, where the increase in the gradient towards the moving wall can be seen, indicating the formation of a 'slip' or 'Knudsen' layer.

4. MEASURED VISCOSITY AND THERMAL CONDUCTIVITY

The shear stress in each cell was determined by sampling the particle velocities. Thus

$$\tau_{meas} = \rho < c_x c_y >$$

where $\vec{c} = (c_x, c_y, c_z)$ is the thermal velocity; the angle brackets denote the average over all particles in the accumulated sample. This shear stress is shown in Fig. 5. Each point is a five point average over a length $2.5\lambda_1$. The measured stress is approximately constant near the center of the flow, where the velocity gradient and temperature (and hence theoretical viscosity) are approximately constant. Closer to the moving plate the measured shear stress reduces.

The measured shear stress is compared with the theoretical shear stress $\tau_t = \mu(T)du_x/dy$ in Fig. 6. The results for two values of the viscosity $\mu(T)$, calculated

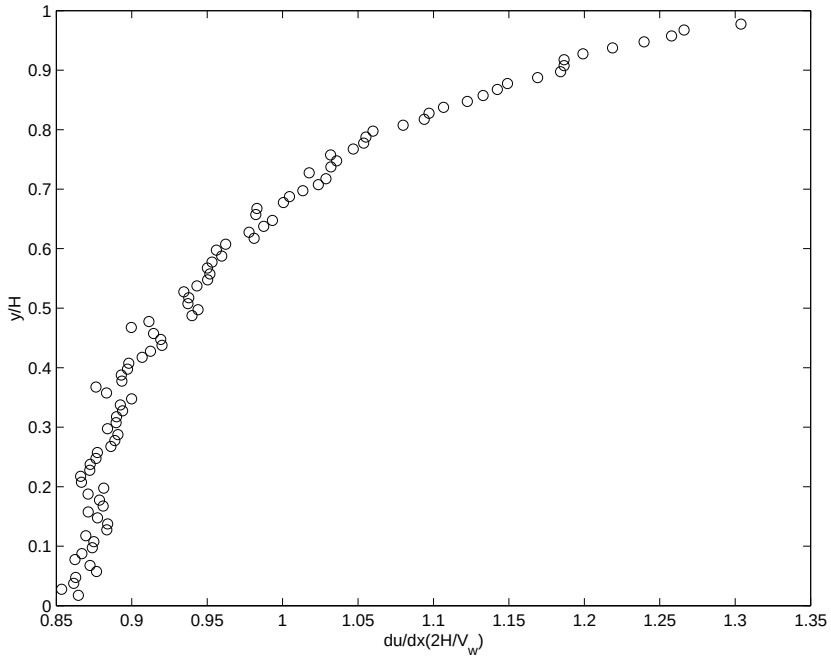

FIG. 4. Velocity gradient in Couette flow, corresponding to Fig. 3. μ-DSMC, Sutherland viscosity law ($T_s = T_1$). $S_w = 3$, $\lambda_1/H = 0.01$. du_x/dy taken from line of best fit to u_x values over 5 adjacent cells. For clarity, only 1 in 2 points shown.

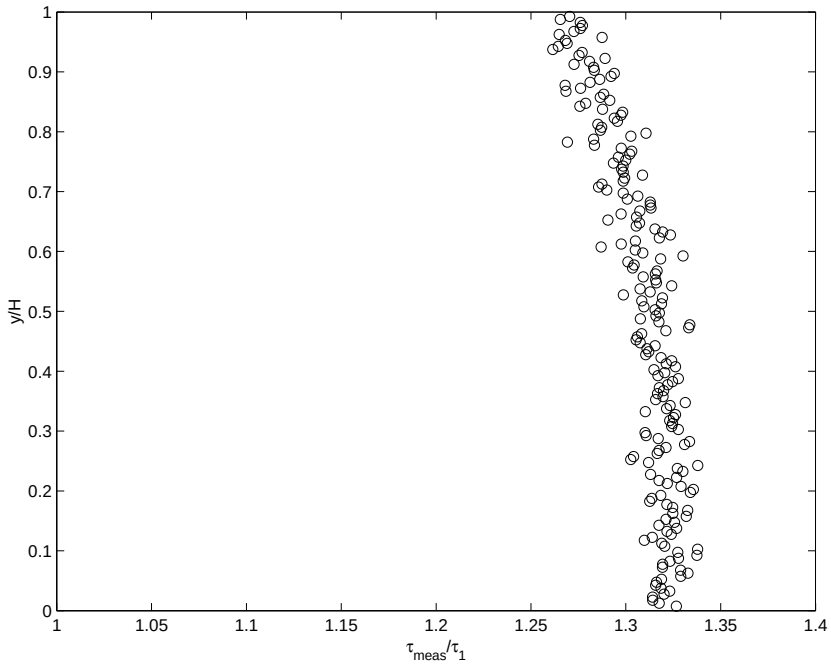

FIG. 5. Shear stress $\tau_{meas} = \rho < c_x c_y >$, calculated from the velocity distribution in each cell. Reference shear stress $\tau_1 = \mu_1 V_w/(2H) = \rho_1 \bar{c}_1 V_w \lambda_1/(4H)$. μ-DSMC, with Sutherland viscosity. Flow conditions and smoothing as in Fig. 3.

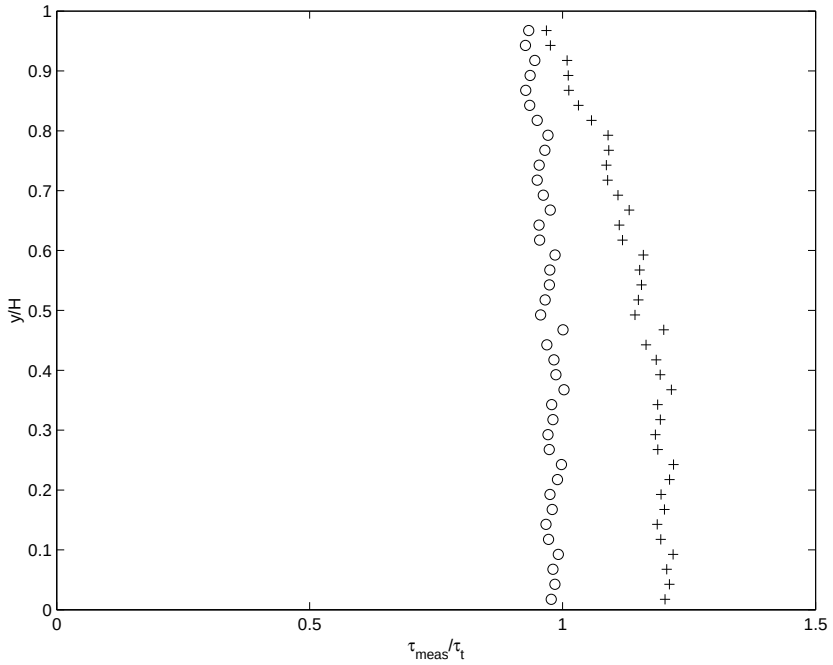

FIG. 6. Shear stress from μ-DSMC simulation with Sutherland viscosity law. τ_{meas} as in Fig. 5. Theoretical shear stress $\tau_t = \mu \frac{du_x}{dy}$. $\frac{du_x}{dy}$ as in Fig. 4. Two viscosity laws: $\circ$, Sutherland viscosity, Eq. 1; $+$, $\mu(T) = \mu_1 (T/T_1)^{\frac{1}{2}}$ (hard sphere). T as in Fig. 3. For clarity, only 1 in 5 points shown.

from the flow temperature, are shown: the Sutherland viscosity law (Eq. 1), which was specified for the μ-DSMC simulations, and the hard sphere law $\mu \propto T^{\frac{1}{2}}$. The results ($\tau_{meas}/\tau_t \approx 1$) show that μ-DSMC reproduces the Sutherland viscosity law as required.

A similar procedure was used to check the thermal conductivity in the simulations. The y-component of the heat transfer vector was calculated as

$$q_{y,meas} = \frac{1}{2}\rho < c_y \vec{c} \cdot \vec{c} >,$$

values of which are shown in Fig. 7. The heat transfer approaches zero at the plane of skew symmetry and a maximum value near the moving plate, as expected. The theoretical value of heat transfer

$$q_{y,t} = -K\frac{dT}{dy} = -\mu \frac{C_p}{\mathrm{Pr}} \frac{dT}{dy}$$

was calculated for the Sutherland viscosity law and the hard sphere law. The measured and theoretical values are compared in Fig. 8; the results show the heat transfer coefficient follows the Sutherland law. Because of the low values of heat transfer and temperature gradient near the axis, the results for $y/H < 0.3$ show increasing scatter and are not shown. This scatter can not be attributed to the special procedures used in μ-DSMC. Bird [2] found a similar 'hopelessly erratic' scatter for a similar flow, using standard DSMC and the VHS collision model.

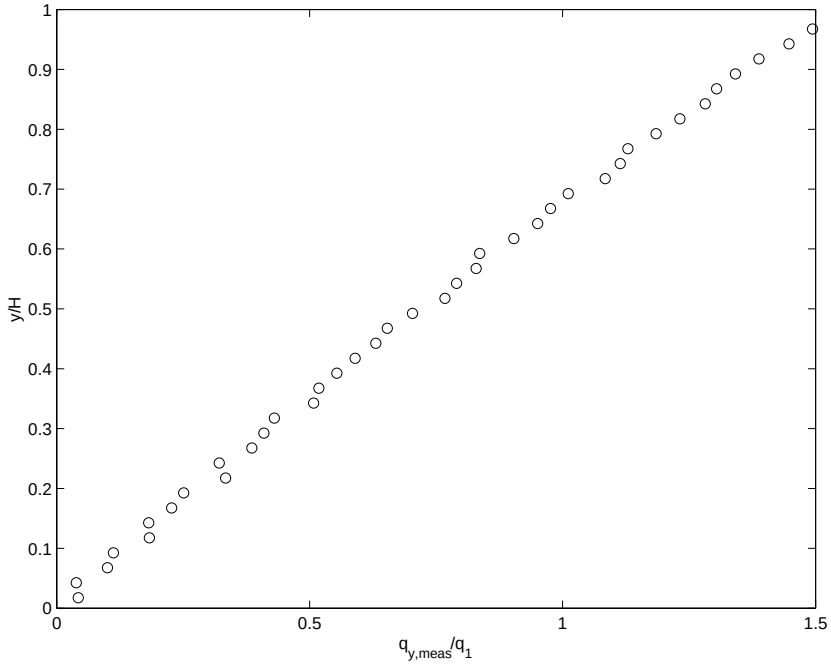

FIG. 7. Heat transfer $q_{y,meas} = -\frac{1}{2}\rho < c_y \vec{c} \cdot \vec{c} >$ from μ-DSMC simulation, calculated from the velocity distribution in each cell. Reference heat transfer $q_1 = \mu_1 \frac{C_p}{\mathrm{Pr}} \frac{T_1}{H}$. $C_p = 5R/2$, Pr = 2/3. Smoothing as in Fig. 3. For clarity only 1 in 5 points shown.

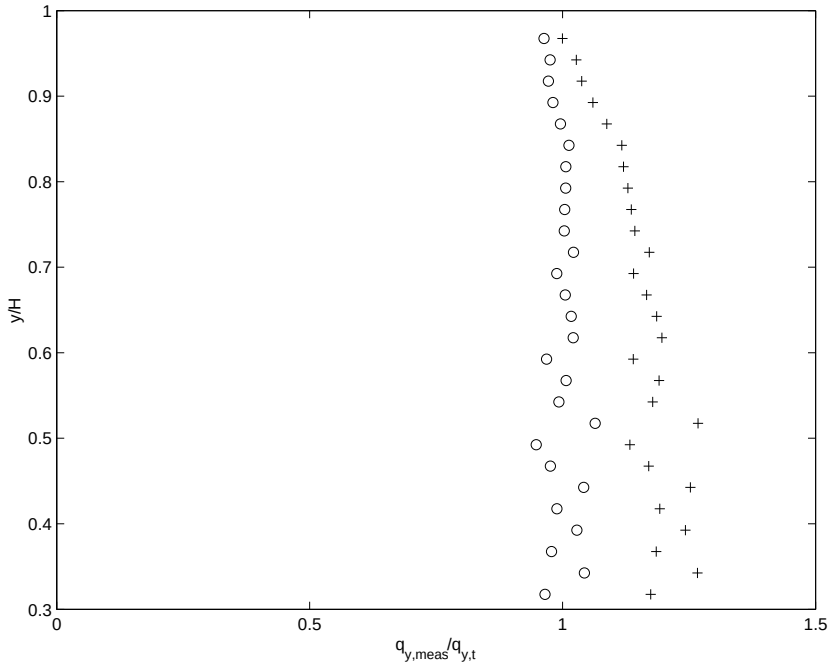

FIG. 8. Heat transfer from μ-DSMC simulation with Sutherland viscosity law. $S_w = 3$, $\lambda_1/H = 0.01$. $q_{y,meas}$ as in Fig. 7. Theoretical heat transfer $q_{y,t} = \mu \frac{C_p}{\mathrm{Pr}} \frac{dT}{dy}$. $C_p = 5R/2$, Pr = 2/3. Two viscosity laws: ∘, Sutherland viscosity, Eq. 1; +, $\mu(T) = \mu_1 (T/T_1)^{\frac{1}{2}}$ (hard sphere). T as in Fig. 3. For clarity, only 1 in 5 points shown.

5. μ-DSMC WITH 'SOFT' COLLISION PROBABILITIES

At high collision energies the collision probability of real molecules is more accurately represented by the variable total cross-section of an inverse power potential, $U(r) \propto 1/r^{\alpha}$. To account for this the VHS (rather than the hard sphere) collision cross-section can be used as the basis of the new method, while still achieving *any* viscosity law. In standard VHS the collision cross-section varies with collision speed as

$$\sigma(g) = \sigma_r (g_r/g)^{2\upsilon} \tag{4}$$

where g_r and σ_r are constant throughout the flow. All that is required to achieve an arbitrary viscosity law is to make σ_r vary from cell to cell as a function of the required viscosity. Thus, with

$$\sigma_r\left(\bar{T}\right) = \frac{15\pi^{\frac{1}{2}}}{16\Gamma\left(4-\upsilon\right)} \frac{m g_r}{\mu\left(\bar{T}\right)}. \tag{5}$$

where $g_r = \left(4R\bar{T}\right)^{\frac{1}{2}}$ and $\bar{T}$ is the time-averaged cell temperature, the standard DSMC procedures will produce the required viscosity $\mu\left(\bar{T}\right)$. The distribution of relative speeds in collisions will be $\propto g^{1-2\upsilon}$.

In order to test μ-DSMC, with this collision probability, in a highly non-equilibrium flow, the structure of a plane 1-D shock was calculated and cpmpared with the shock structure calculated with the GHS model of Hash and Hassan [9].

6. GENERALIZED HARD SPHERE

The GHS collision model [9] uses hard sphere scattering and a total collision cross-section made up of any number of VHS cross-sections. Here we use

$$\sigma/\sigma_0 = \phi\left(g_0/g\right)^{2\upsilon_1} + \left(1-\phi\right)\left(g_0/g\right)^{2\upsilon_2} \tag{6}$$

where σ_0 is a reference cross-section, $g_0 = \left(4RT_0\right)^{\frac{1}{2}}$ and T_0 is a reference temperature. The Chapman-Enskog viscosity for this cross-section, (and isotropic scattering), is

$$\mu = \frac{15\pi^{\frac{1}{2}}}{16\Gamma\left(4-\upsilon_1\right)} \frac{\left(T/T_0\right)^{\frac{1}{2}+\upsilon_1}}{\left[\phi+(1-\phi)S\right]} \frac{m g_0}{\sigma_0}. \tag{7}$$

where

$$S = S_0\left(T_0/T\right)^{\upsilon_2-\upsilon_1}.$$

With $\upsilon_1 = 2/13$, $\upsilon_2 = 14/13$ and $\phi = 0.61$, Eq. 7 can give a reasonably good representation of the viscosity of argon, for which $m = 66.3\times10^{-27}$ kg (see Fig. 9). The cross-section $\sigma_0 = 6.457\times10^{-19}\mathrm{m}^2$ follows from Eq. 7 with $\mu_0 = 2.272\times10^{-5}$ $\mathrm{Nm}^{-1}\mathrm{s}^{-1}$ and $T_0 = 300$ K. The GHS viscosity is 5% greater than the experimental data at $T = 1500$ K.

For low temperatures, the GHS collision model is extremely computationally inefficient; the collision probability increases dramatically for collision speeds $g <<$

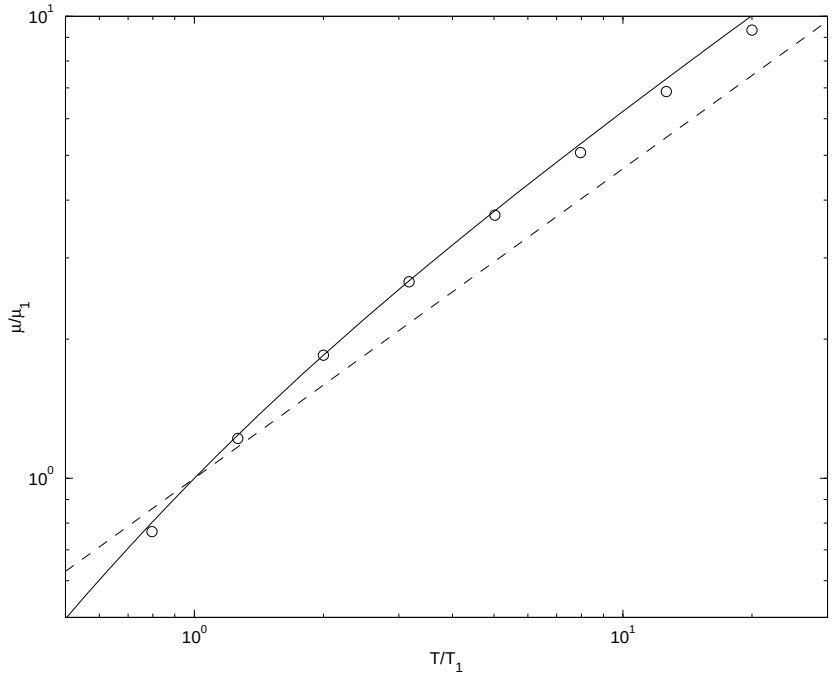

FIG. 9. Viscosity μ/μ_1 *vs.* T/T_1: ——, generalized hard sphere model (Eq. 7) with $\upsilon_1 = 2/13$, $\upsilon_2 = 14/13$, $\phi = 0.61$, $\sigma_0 = 6.457 \times 10^{-19}$ m^2, $T_0 = 300$ K; ∘, argon data Kestin *et al.* [10]; $\cdots$, $\mu = \mu_1(T/T_1)^{0.67}$. $T_1 = 150$ K, $\mu_1 = 1.237 \times 10^{-5}$ Nm^{-1}s^{-1}.

$(4RT_0)^{\frac{1}{2}}$ so that an overwhelming number of low energy collisions must be calculated. However, these low energy collisions make an insignificant contribution to the viscous behavior of the model. To overcome this, we can assume that the collision probability is constant for $g < (2RT_1)^{\frac{1}{2}}$ where T_1 is the lowest temperature in the flow (the pre-shock temperature in the simulations which follow). It can be shown that this modification affects the theoretical viscosity only at very low temperatures; the deviation from the viscosity law of Eq. 7 is approximately 1.3% at $T = T_1$ and reduces dramatically for $T > T_1$.

7. PLANE 1D SHOCK

The FORTRAN computer code DSMC1S, supplied by Bird [2], which calculates the internal structure of a plane 1D shock was modified to include the GHS collision model and μ-DSMC. The μ-DSMC procedure was based (locally) on the VHS cross-section, with $\upsilon = 1/6$. The specified viscosity law for μ-DSMC was that of the GHS model (Eq. 7).

Simulations were also undertaken with the standard VHS collision model with $\upsilon = 1/6$ for which the viscosity is proportional to $T^{0.67}$; this viscosity law is also shown in Fig. 9. In order to accentuate the difference between the VHS viscosity and the GHS/μ-DSMC viscosity, the pre-shock temperature T_1 was set at 150 K. All three models had the same viscosity μ_1 upstream of the shock and the length scale in all the profiles shown below is the nominal mean free path $\lambda_1 = 2\mu_1/(\rho_1 \bar{c}_1)$. The simulation flowfield typically spanned a length of $30\lambda_1$. 200 cells were used, with 6 sub-cells per cell. The cell size was typically $< 0.75\lambda_2$ where λ_2 is the nominal mean

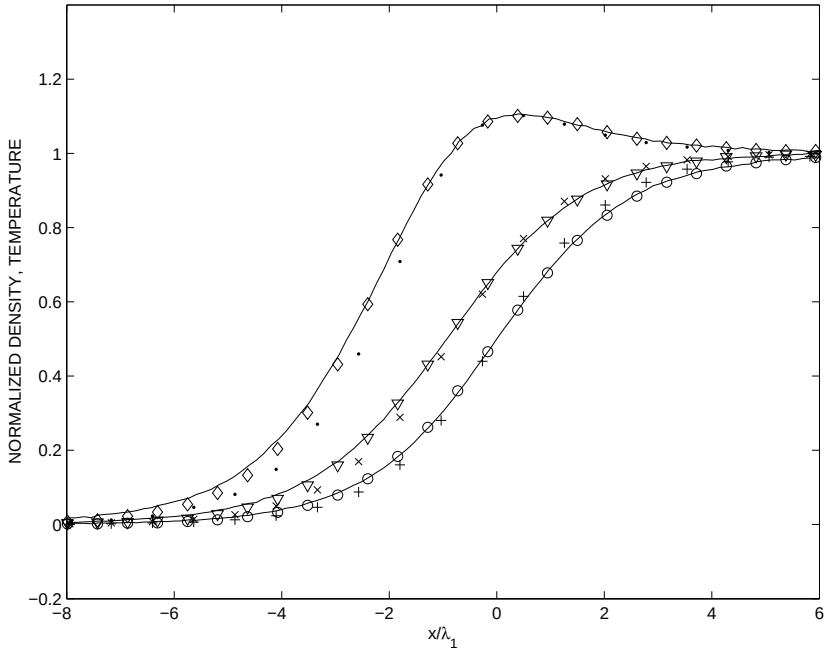

FIG. 10. Normalized density and temperatures for normal shock ($M_1 = 2$, $T_1 = 150$K, $\gamma = 5/3$). μ-DSMC and VHS collision model compared to GHS collision model. Solid lines show the results for the GHS collision model. Closed symbols, μ-DSMC: $\circ$ ρ', ∇ T'_x, $\diamond$ T'_p. Closed symbols, VHS collision model ($\upsilon = 1/6$): $+$ ρ', $\cdot$ T'_x, $\times$ T'_o. Every 3^{th} point only shown. Theoretical viscosities shown in Fig. 9.

free path downstream of the shock. The time step was $\Delta t = 0.2\lambda_1/\bar{c}_1$. Translational degrees of freedom only were considered, giving a ratio of specific heats of $\gamma = 5/3$. Results for three shock Mach numbers are presented: $M_1 = 2$, 4 and 8, for which the temperature ratio across the shock is $T_2/T_1 \approx 2$, 5.9 and 20.9 respectively.

Fig. 10 shows the temperature and density profiles obtained for the Mach 2 shock using the new simulation method, compared with the GHS model. The flow properties are normalized as

$$\rho' = (\rho - \rho_1)/(\rho_2 - \rho_1),\ \ T'_x = (T_x - T_1)/(T_2 - T_1),\ \ T'_o = (T_o - T_1)/(T_2 - T_1)$$

where T_x is the x-component of kinetic temperature in each cell, $T_o = (T_y + T_z)/2$ is the 'orthogonal' temperature, and $T_{1/2}$ is the equilibrium temperature upstream or downstream. The origin of the x-axis is set at the point where $\rho' = 0.5$. The viscosity law in both cases is the same, and the μ-DSMC results agree closely with the GHS results. The temperature rise ahead of the shock is slightly less severe for μ-DSMC than for the GHS model.

Figs. 11 and 12 show similar results for shock Mach numbers of $M_1 = 4$ and 8. Also shown are the results for the VHS collision model. Because of the lower viscosity through the shock for this model, the shock thickness is smaller, and the profiles differ noticeably from those for the GHS and μ-DSMC models. In other words, although the μ-DSMC model uses the VHS collision probability locally in each cell, it matches the behaviour of the GHS model, because its viscosity (and hence collision rate) is similar.

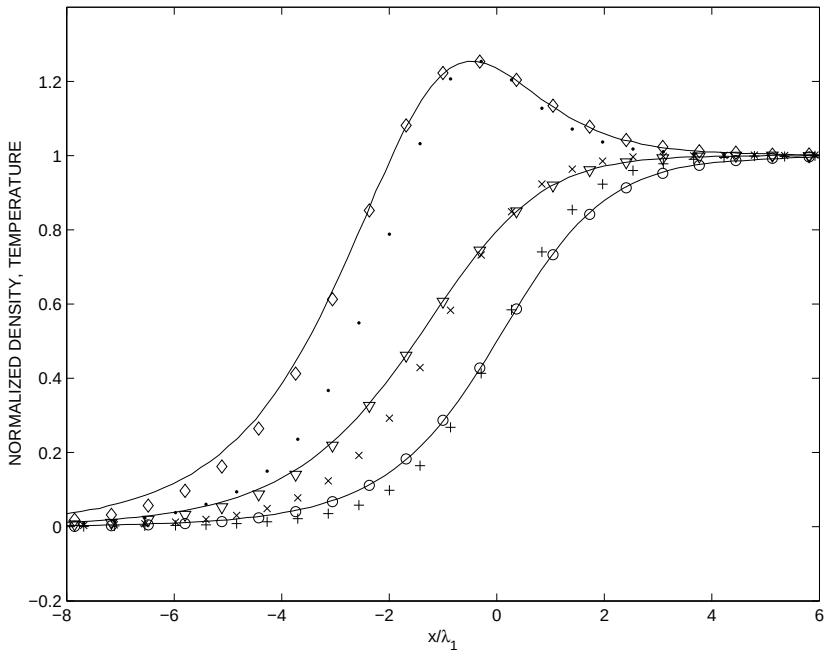

FIG. 11. Normalized density and temperatures for normal shock ($M_1 = 4$, $T_1 = 150$ K, $\gamma = 5/3$). μ-DSMC (closed symbols) and VHS collision model (open symbols) compared to GHS collision model (solid lines). Symbols as in Fig. 10.

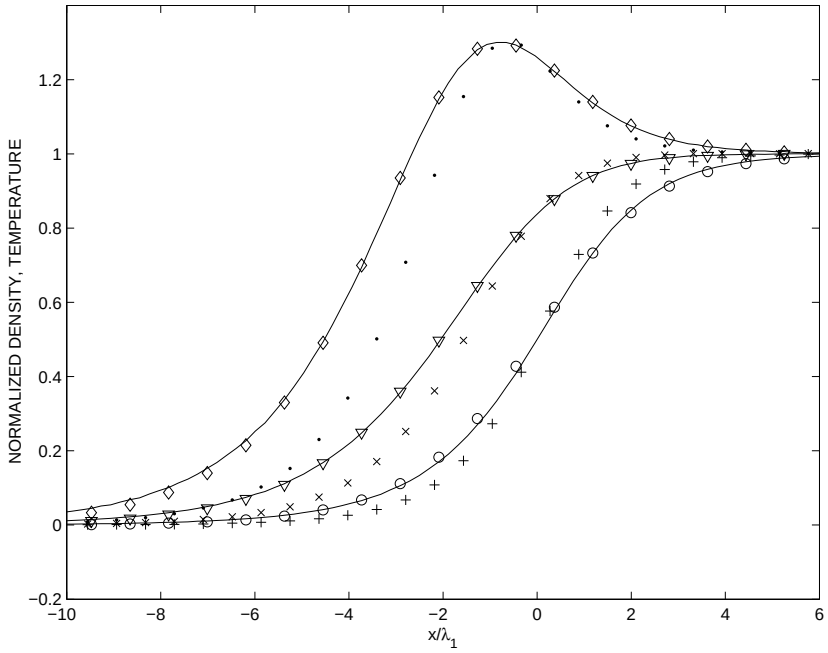

FIG. 12. Normalized density and temperatures for normal shock ($M_1 = 8$, $T_1 = 150$ K, $\gamma = 5/3$). μ-DSMC (closed symbols) and VHS collision model (open symbols) compared to GHS collision model (solid lines). Symbols as in Fig. 10.

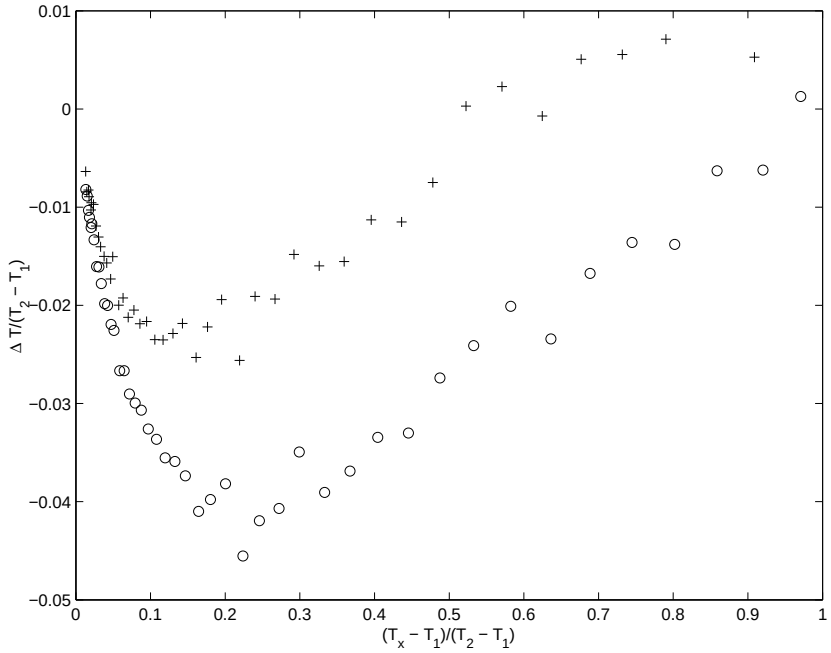

FIG. 13. Deviation $\Delta T_x/(T_2-T_1)$ between μ-DSMC and the GHS collision model ($M_1 = 4$): ∘, standard μ-DSMC (see Fig. 11) maximum deviation $\Delta T/(T_2 - T1) = 4.6\%$; +, modified μ-DSMC (see Fig. 14) maximum deviation $\Delta T/(T_2 - T1) = 2.6\%$.

8. MODIFIED μ-DSMC

Figs. 10, 11 and 12 indicate that μ-DSMC matches the results of the GHS model very closely for highly non-equilibrium flow in the interior of the shock. The only small difference lies in a slightly steeper profile of the temperature T_x. For example, Fig. 13 shows the difference ΔT in the value T_x, as calculated by μ-DSMC, and the value of T_x as calculated with the GHS model, normalized with respect to the temperature rise across the shock $T_2 - T_1$, for the Mach 4 shock. The maximum difference is 4.6%. For $M_1 = 2$ and $M_1 = 8$ the maximum difference is 2.8% and 1.6% respectively.

Although this deviation is probably insignificant μ-DSMC can be modified to reduce this particular difference. All that is required is to base the reference collision cross-section in any cell, not on the kinetic temperature but on the maximum component of kinetic temperature, in this case T_x. Thus, in place of Eq. 5, we can use

$$\sigma_r\left(T_{max}\right) = \frac{15\pi^{\frac{1}{2}}}{16\Gamma\left(4-\upsilon\right)}\frac{mg_r}{\mu\left(T_{max}\right)}, \tag{8}$$

where $T_{max} = \max\left(\bar{T}_x, \bar{T}_y, \bar{T}_z\right)$. As before, $\bar{T}$ denotes the time-averaged temperature in any cell. The shock structure calculated with 'modified' μ-DSMC is shown in Fig. 14. It can be seen that the agreement with the GHS results is slightly better than that shown in Fig. 11. Fig. 13 shows the maximum deviation between the T_x profiles for the modified and unmodified version of μ-DSMC; the maximum deviation is reduced from 4.6% to 2.6%. The density and T_o profiles are changed by insignificant amounts. Similar results were found for $M_1 = 2$ and 8; the modified

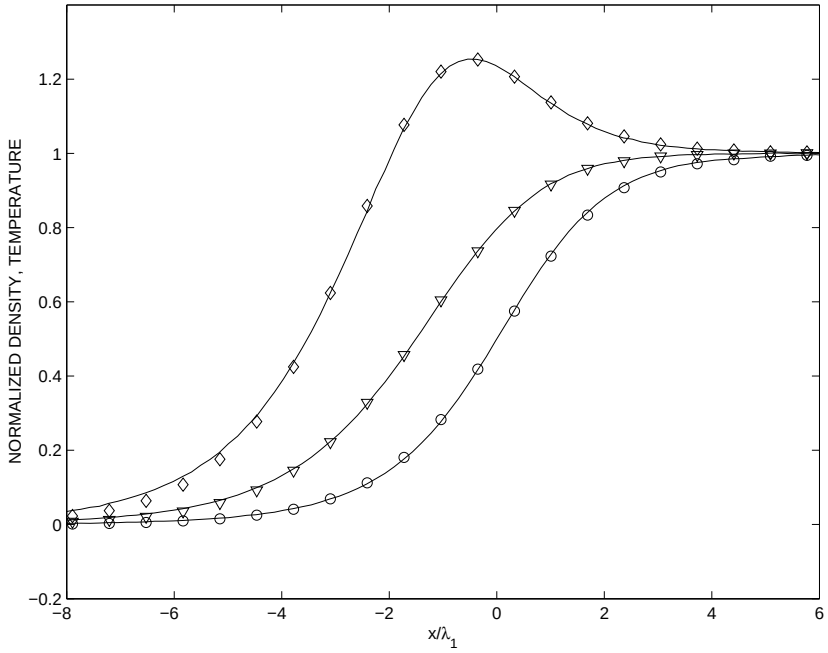

FIG. 14. Normalized density and temperatures for normal shock ($M_1 = 4$, $T_1 = 150$ K, $\gamma = 5/3$). Modified μ-DSMC (closed symbols) compared to GHS collision model (solid lines). Symbols as in Figs. 10. Max deviation reduced from 4.6% to 2.6%.

μ-DSMC results showed that the maximum deviation of T_x from the GHS profiles was reduced from 2.8% to 1.6% and 1.6% to 1.3%, respectively.

Plausible reasons can be given to justify this modification: The simulation collision rate for the GHS simulations within the shock is slightly less than that expected for equilibrium conditions. The collision rate is lower because, when $T_x > T_{kin}$ the average collision speed is greater than the average collision speed at equilibrium. The larger collision speed leads to a smaller average collision cross-section, and larger average mean free path, within the shock. Hence the flow is more 'dissipative' than might be expected from equilibrium assumptions. Using the maximum component of kinetic temperature to calculate the required viscosity mimics this effect. Wherever the three components of kinetic temperature are significantly different a smaller reference cross-section is used in each cell and the collision rate is slightly reduced.

9. NUMBER OF SIMULATOR PARTICLES

In a typical DSMC application as few as 10 simulator particles per cell might be used. Since the cell temperature (and hence the effective collision cross-section) must be estimated from this small number of particles, it might seem that μ-DSMC would be sensitive to the number of simulator particles used. On the other hand, the time-averaged temperature is used and this quickly becomes independent of the instantaneous number of simulators in any cell for steady flow.

The effect of varying the number of simulator particles was found by repeating the 1D shock calculations. Five cases were considered; the number of particles per cell in the upstream flow was 122, 61, 30, 15 and 7. In the last case, before steady

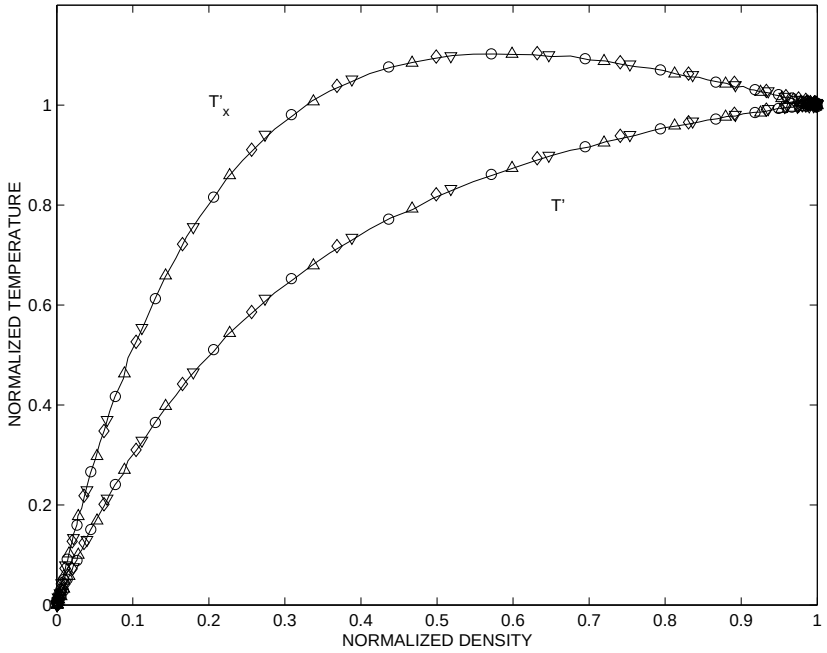

FIG. 15. Effect of number of simulator particles/cell on the final time-averaged steady state. Temperature *vs.* density through the shock. Normalized values: $T'_x = (T_x - T_1)/(T_2 - T_1)$, $T = (T - T_1)/(T_2 - T_1)$, $\rho' = (\rho - \rho_1)/(\rho_2 - \rho_1)$. $M_1 = 2$, Modified μ-DSMC. Particles/cell in upstream flow: —-, 122; ∘, 61; △, 30; ◇,15; ∇, 7. One in five points only shown for clarity.

state was reached, fewer than 3 particles were occasionally found in some cells. In that case, a new cell temperature was not calculated, but the previous estimate was used. In all cases the simulation continued until the final sample sizes were the same. The time-averaged profiles of T_x and T are shown in Fig. 15. These are for modified μ-DSMC which, since it uses only one component of kinetic temperature to set the average cross-section, might be expected to suffer more from small sample sizes. The results are virtually independent of the number of simulator particles used. The time-average collision rate differed for the five cases by less than 1% in the interior of the shock.

10. DISCUSSION

The approach taken here to achieve an arbitrary viscosity, appears to be simpler than that taken by Koura and Matsumoto [12], by which they make the two disposable parameters of the VSS model empirical functions of the collision energy and these parameters have to be numerically determined. It is important that the standard Borgnakke-Larsen [4] energy exchange model for molecules with translational and vibrational degrees of freedom can be used with μ-DSMC; this is because μ-DSMC, is based on the hard sphere or variable hard sphere collision probability within each cell.

There are some parallels between the new method and the method of Garcia *et al.* [8], which was originally designed to obtain a dense gas equation of state. In that method, the transport properties are altered by adding a random displacement between the collision partners, and it appears this could be done while retaining

the perfect gas equation of state of standard DSMC. In order to obtain an arbitrary viscosity law, the magnitude of this random displacement has to depend on the flow temperature, and in this respect would be similar to μ-DSMC; that is, the collision process would not depend only on the magnitude of relative velocity in a particular collision, but also on the velocities of all the potential collision partners in the cell through the kinetic temperature.

I previously proposed a method [14], 'collision rate DSMC' (ν-DSMC) in which all collision speeds in a cell were equally likely (a Maxwell total cross-section) but which achieved a realistic viscosity law by calculating the collision rate from the required viscosity law and the kinetic temperature in the cell. That method was shown to give results within about 5% of the standard VHS collision model (when the viscosities were matched) for a number of typical non-equilibrium flows, with a computational effort of about 50-80% of that required for the VHS model. μ-DSMC, requires the same computational effort as the standard VHS model, but improves on ν-DSMC in two related ways - the distribution of relative velocities in collisions is more realistic, and the non-equilibrium collision rate depends on the local distribution of particle velocities as well as the kinetic temperature.

The extra computational effort required for μ-DSMC, compared to the VHS model, for the simulations reported here, was negligible, consisting only of calculating the time-averaged components of kinetic temperature. The samples required to do this are accumulated in standard DSMC in order to obtain the final steady state temperature. For unsteady flow it might be necessary to calculate the kinetic temperature at every time step, and tests of this showed that the computational load might increase by about 10%, in that case.

If the diffusion coefficient (or Schmidt number) is deemed important for any particular flow the variable soft sphere (VSS) collision model introduced by Koura and Matsumoto [11] [12] can be used as the basis of μ-DSMC. In its basic form the VSS model displays a power law viscosity the same as the VHS model, but the diffusion coefficient is adjustable.

11. SUMMARY

μ-DSMC is a new simulation method for rarefied flows by which an arbitrary viscosity law can be implemented. It is as simple as standard DSMC using the VHS collision model and the computational burden required to achieve an arbitrary viscosity law is negligible.

Numerical tests for high speed Couette flow, using hard sphere collision probabilities have shown that the coefficients of viscosity and thermal conductivity can be made to follow the Sutherland law. Further tests for the highly non-equilibrium flow within a normal shock, using VHS collision probabilities, and a viscosity law matching the GHS viscosity law, have shown that the μ-DSMC results are negligibly different from those obtained with the more complex GHS model. Using μ-DSMC there is no need to construct a realistic collision model, or use a realistic intermolecular potential, in order to obtain a viscosity law which matches the experimental data to a certain accuracy; the best experimental data can be used directly to specify the collision cross-section in each cell.

REFERENCES

1. G. A. Bird. Monte-Carlo simulation in an engineering context. In S. Fisher, editor, *Rarefied Gas Dynamics*, New York, U.S.A., 1981. AIAA.
2. G. A. Bird. *Molecular Gas Dynamics and the Direct Simulation of Gas Flows*. Clarendon, Oxford, 1994.
3. C. Borgnakke and P. S. Larsen. Statistical collision model for Monte-Carlo simulation of polyatomic gas. Technical Report AFM 73-08, Dept, Fluid Mechanics, Technical University of Denmark, Lyngby, Denmark, 1973.
4. C. Borgnakke and P. S. Larsen. Statistical collision model for Monte-Carlo simulation of polyatomic gas mixture. *J. Comp. Phys.*, 18:405, 1975.
5. S. Chapman and T. G. Cowling. *The mathematical theory of non-uniform gases*. CUP, Cambridge, 3rd edition, 1970.
6. J. Davis, R. G. Dominy, J. K. Harvey, and M. N. Macrossan. An evaluation of some collision models used for Monte-Carlo calculation of rarefied hypersonic flows. *J. Fluid Mech.*, 135:355–371, 1983.
7. A. I. Erofeev and V. A. Perepukhov. Hypersonic rarefied flow about a flat plate by the Direct Simulation Method. In Camprague, editor, *Rarefied Gas Dynamics*, page 417, Paris, France, 1979. C.E.A.
8. A. L. Garcia, F. J. Alexander, and B. J. Alder. A particle method with adjustable transport properties - the generalized consistent Boltzmann algorithm. *J. Stat. Phys.*, 89:403 – 409, 1997.
9. D. B. Hash and H. A. Hassan. A generalized hard-sphere model for Monte-Carlo simulation. *Phys. Fluids A*, 5(3):738 – 744, March 1993.
10. J. Kestin, K. Knierim, E. A. Mason, B. Najafi, S. T. Ro, and M. Waldman. Equilibrium and transport properties of the noble gases and their mixtures at low density. *J. Phys. Chem. Ref. Data*, 13(1):229–303, 1984.
11. K. Koura and H. Matsumoto. Variable soft-sphere molecular model for inverse-power or Lennard-Jones potential. *Phys. Fluids A*, 3:2459 – 2465, 1991.
12. K. Koura and H. Matsumoto. Variable soft-sphere molecular model for air species. *Phys. Fluids A*, 4:1083 – 1085, 1992.
13. P. I. Larsen and C. Borgnakke. Statistical collision model for simulating polyatomic gas with restricted energy exchange. In Becker and M. Fiebig, editors, *Rarefied Gas Dynamics*, Porz-Wahn, Germany, 1974. DFVLR press.
14. M. N. Macrossan. ν-DSMC: a fast simulation method for rarefied flow. *J. Comput. Phys*, 173:600–619, 2001.